Proceedings World Geothermal Congress 2015
Melbourne, Australia, 19-25 April 2015

Scale Inhibition at the Soultz-sous-Forêts (France) EGS Site: Laboratory and On-Site Studies

Julia Scheiber, Andrea Seibt, Johannes Birner, Albert Genter, Nicolas Cuenot and Wilfried Moeckes

[1]GEIE, “Exploitation Minière de la Chaleur”, Route de Soultz, 67250 Kutzenhausen, France

[2]BWG Geochemische Beratung GmbH, Seestraße 7A, 17033 Neubrandenburg, Germany

[3]GTN Geothermie Neubrandenburg GmbH, Seestraße 7A, 17033 Neubrandenburg, Germany

scheiber@soultz.net

Keywords: barite, scaling, NORM, radiation protection, scale inhibitor, phosphonic acid, EGS

ABSTRACT

Scale formation in the surface and subsurface installations of the Soultz geothermal power plant affect negatively operational performance of the geothermal cycle. For reasons of safety at work and long term power plant operation, the formation of barite needs to be inhibited continuously. Therefore, several inhibitor products, based on phosphonic acids, were tested in laboratory experiments. This study included laboratory tests for calcium tolerance, effectiveness and dose rate adjustment by tube blocking tests with artificial and original Soultz brine. Based on the performance during the tests, one product showed the best results for barite inhibition at the Soultz site and was consequently selected for additional laboratory tests which investigated long-term efficiency, thermal stability and reservoir rock/inhibitor interactions. The inhibitor suppressed successfully barite formation for 24 h at 90°C in contact with reservoir rock material. Small scale laboratory tests were found to be simple but powerful tools for inhibitor selection, efficiency tests and dose rate adjustment before inhibitor on-site application.

Geothermal fluids trapped within deep-seated fractured crystalline rocks from the Upper Rhine Valley must be carefully investigated in order to minimize scaling (sulfate, sulfide) and seriously limit the natural radioactivity associated with. At the Soultz site an inhibitor injection system was designed, installed and tested for continuously inhibitor injection. The on-site efficiency test showed very promising results during the short-time test for barite scale mitigation.

1. INTRODUCTION

The geothermal power plant of Soultz-sous-Forêts is located in the NE of France, 50 km NE of Strasbourg, at the western rim of the Upper Rhine Graben (URG). The project started in 1987, with the aim to develop heat exploitation of deep reservoirs in hot dry rocks (HDR) by creating an artificial deep heat exchanger in a closed environment, Gérard and Kappelmeyer (1987). Therefore, one exploration well, EPS-1, and four deep wells, GPK-1 to GPK-4, were drilled between 1987 and 2005 down to the crystalline basement of the Rhine Graben. During drilling and well testing it became obvious that native brine was circulating through the fracture network of the naturally fractured granite, Genter and Traineau (1992), Genter et al. (2010). The original HDR design was found to be obsolete. Nevertheless, permeability of the reservoir decreased with increasing depth and the initially low permeability was improved by several hydraulic and chemical stimulations, creating an Enhanced Geothermal System (EGS), Gérard et al. (2006).

The Soultz EGS site operates a naturally fractured granitic reservoir percolated by Na-Cl-Ca brine with Total Dissolved Solids (TDS) up to 100 g/L. Geothermal brine is produced at 160°C/20 bars and is reinjected at 70°C/18 bars. For power production an Organic Rankine Cycle (ORC) was designed and installed between 2007 and 2009 with an estimated gross capacity of 2.2 MWe. Due to temperature decrease of 90 K in the ORC unit, strontium rich barite ($Ba_{0.6}Sr_{0.4}SO_4$) becomes oversaturated and forms a homogenous scaling layer. Additionally, minor amounts of sulfide minerals like galena (PbS) and As, Sb, Fe-mixed sulfides are present.

Several issues are connected with scale formation at the Soultz site. Firstly, those scales form an insulation layer inside of the heat exchanger tubes and decrease thereby efficiency of heat transfer from the geothermal to the organic fluid. In consequence, cleaning operations for scale removal are required in regular time intervals to keep up efficiency of energy production. Secondly, the scales have to be classified as NORM (Naturally Occurring Radioactive Material) related to the presence of Ra-226 and Pb-210, incorporated by chemical substitution in the scales. Therefore, cleaning and disposal operations require radiation protection regulations for workers based on French regulations. Thirdly, the inner diameter of the reinjection wells decreases slowly but continuously by deposition of scales. Recently, well loggings proofed the existence of a progressing precipitation front versus depth inside of the injection wells which can reach the open-hole section as a function of injected brine volume and injection temperature.

In order to keep up long-term efficiency of both, the geothermal power plant and the geothermal loop and out of reasons of safety at work an intensive inhibitor study was launched for barite scale mitigation. This study also investigated the question whether or not small scale laboratory experiments can be eligible for chemical selection and dose-rate adjustment for on-site application. All products tested were based on phosphonic acid which is already successfully applied for barite scale mitigation in the hydrocarbon industry.

2. GEOCHEMISTRY OF THE SOULTZ BRINE AND SCALE CHARACTERIZATION

2.1 Physico-chemical parameters of Soultz brine and gas samples

The Soultz geothermal brine shows very similar chemical composition between 1200 and 5000 m depth except for some minor electrolytes which are influenced by temperature dependent mineral saturation state like barite and amorphous silica, Pauwels et al. (1991), Pauwels et al. (1993), Aquilina et al (1997), Sanjuan et al. (2010) and Sanjuan et al. (2011). Total Dissolved Solids (TDS) are close to 100 g/l and are dominated by Na-Cl-Ca. Brine pH of 5 is slightly acidic and brine is produced under strictly anoxic conditions and low Eh values.

2.1.1 Brine sampling

Brine was sampled 2011 and 2013 from GPK-2 (production) and GPK-3 (injection) by using a small scale tubular water cooling device which was connected by coiled tubing to the surface installations. Sampling temperature was adjusted in 2011 to approximately 60°C and in 2013 to approximately 20°C for both, production and injection side. Coiled tubing and cooling device were rinsed more than 30 min until constant pH, Eh and conductivity values were reached. In 2011 no inhibitor was utilized during brine sampling, in 2013 a continuous injection of a phosphonic acid based product was applied. Conductivity, pH and Eh were measured continuously in a flow-through cell made of plexiglass. Soft degassing was observed in this cell due to the pressure release below 2 bars.

Figure 1 shows the evolution of stable sampling conditions as a function of time during the 2013 brine sampling at the production side (left) and at the reinjection side (right). Every slight change of temperature results immediately in a response of the pH and Eh sensors. At both sides of the geothermal loop the pH is slightly acidic with values close to 4.8-4.9 whereas the Eh values are higher at the cold side with a difference of more than >100 mV between production and injection side at both sampling campaigns, Table 1. This is very probably related to corrosion and scale formation phenomena at the cold side of the geothermal loop and not to the inhibitor injection.

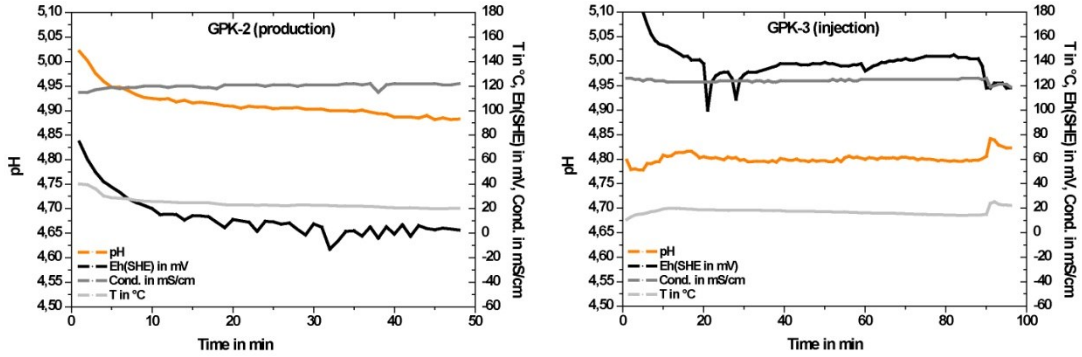

Figure 1: Evolution of conductivity, pH and Eh as a function of time during the 2013 on-site brine sampling at the production side (left) and at the reinjection side (right) in a flow through cell.

Brine was filtered directly after sampling through a 0.45µm cellulose acetate filter. No further treatment for anion analysis was applied, for cation analysis the sample was acidified with nitric acid for sample stabilization. Additionally one brine sample was diluted immediately after filtration to 1:250 and conditioned with r nitric acid for analysis of Ba, Sr and SO4. For analysis of the anions no further treatment was applied after filtration. Table 1 presents full analyses of the physical sampling parameters and the chemical composition of the Soultz brine of the 2011 and 2013 brine sampling which was a part of the barite scale mitigation study. No significant difference between the sampling surveys were observed, also no specific observation was made between fluid samples from the production and the injection side except for the Pb concentration. This fact will be discussed in chapter 4.

Table 1: Soultz geothermal brine composition of 2011 and 2013 sampling campaigns of the production and reinjection wells GPK-2 and GPK-3. Analysis of the 06.02.13 brine samples after Scheiber et al. (2013) and Scheiber et al. (2014).

	$T_{wellh.}$ °C	$T_{sampl.}$ °C	pH	$Eh_{(SHE)}$ mV	Cond. mS/cm	TDS g/l	Alk. mmol/l	Na mg/l	Ca mg/l	K mg/l
GPK-2 06.04.11	157	65	5.06	-106	120	96	2.60	25800	7600	3740
GPK-3 06.04.11	61	61	5.07	46	121	n.d.	3.15	26000	7450	3500
GPK-2 06.02.13	155	20	4.88	5	122	97	3.02	25200	7400	3360
GPK-3 06.02.13	70	22	4.82	117	121	96	3.00	24150	7420	3270
	Sr mg/l	**Li mg/l**	**Mg mg/l**	**Ba mg/l**	**NH_4 mg/l**	**Fe_{total} mg/l**	**Mn mg/l**	**Cs mg/l**	**Rb mg/l**	**As_{total} mg/l**
GPK-2 06.04.11	412	185	141	26	24	35	18	16	26	10
GPK-3 06.04.11	405	182	137	25	26	37	17	n.d	n.d.	10
GPK-2 06.02.13	418	169	142	26	24	30	18	11	24	11
GPK-3 06.02.13	406	169	141	26	24	28	18	11	24	11
	Cl mg/l	**Br mg/l**	**SO_4 mg/l**	**HCO_3 mg/l**	**F mg/l**	**PO_4 mg/l**	**B mg/l**	**SiO_2 mg/l**	**Zn mg/l**	**Pb mg/l**
GPK-2 06.04.11	56000	229	150	159	7	3	39	201	4	0.30
GPK-3 06.04.11	n.d.	n.d.	n.d.	192	n.d.	n.d.	39	191	3	0.35
GPK-2 06.02.13	57300	249	228	184	6	4	41	174	3	0.07
GPK-3 06.02.13	54400	249	208	183	6	5	37	189	2	0.10

2.1.1 Gas Characterization

During brine sampling in 2011 two gas samples were taken to investigate the gas-liquid ratio (GLR) and the gas composition. The GLR was determined to be 0.8 and the gas phase is dominated by 95% CO_2. N_2 and CH4 are present at minor fractions with 4 and 0.4% respectively, Figure 2.

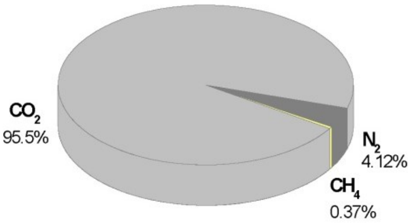

Figure 2: Composition of dissolved gases of the Soultz brine. CO_2 dominates with 95% over N_2 (4%) and CH_4 (< 1%).

2.2 Characterization of the Soultz Scales

Scale formation is directly linked with brine geochemistry and changes of the barite mineral saturation state due to the temperature decrease of 90 K in the heat exchangers. Scales are deposited mainly inside the tubular heat exchanger system, within the equipment downstream to the injection well which comes in contact with brine and even inside of the injection wells, Figure 3.

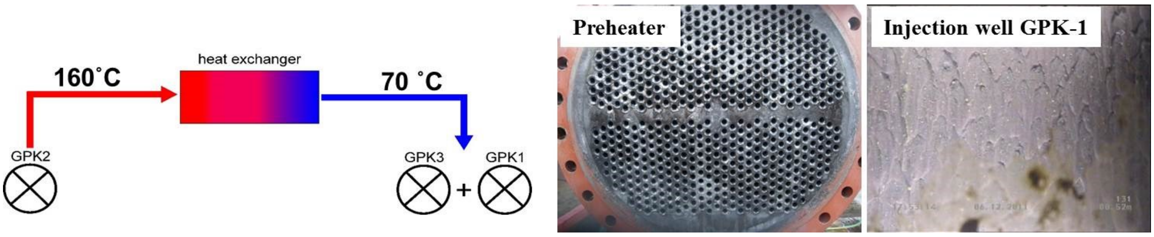

Figure 1: Left: Schematic view of the thermal regime before and after the heat exchanger system at Soultz. Middle: A thin, greyish scale layer cover the complete surface of Preheater 1. Right: Scales cover the inner casing of the injection well GPK-1 in 80 m depth.

An intense study of the ORC heat exchanger scales showed that strontium rich barite ($Ba_{0.6}Sr_{0.4}SO_4$) dominates the scales which also contain a minor fraction of galena (PbS) and trace amounts of mixed sulfides ($(Fe,Sb,As)S_x$), Scheiber et al. (2012) and Nitschke (2012). The morphology of plate like scales, Figure 4a, was investigated by electron microscopy (FEI Quanta 650 FEG ESEM) and EDX (15 kV) for semiquantitative elemental analysis. Fine sulfide crystals cover the dominating barite layer, Figure 4b. The tiny sulfide crystals are enriched in Pb and contain small amounts of As, Fe, Sb and Cu, Figure 4c. Barite crystals are enriched in strontium, forming solid solutions of barite ($BaSO_4$) and celestine ($SrSO_4$), Figure 4d.

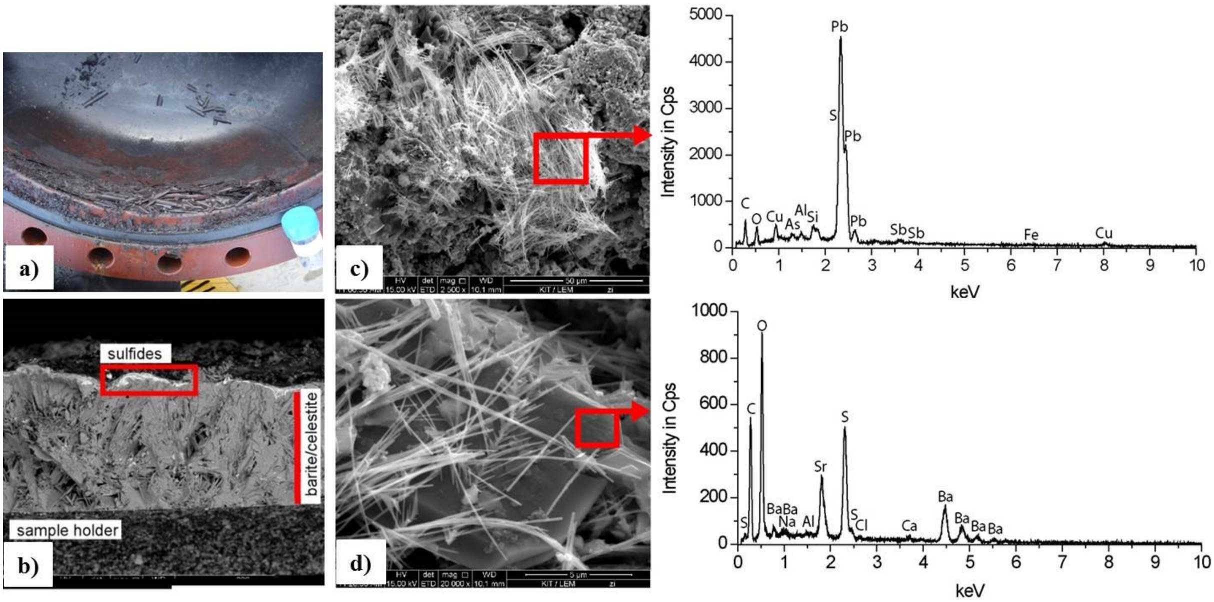

Figure 4: *(a)* Plate like scales cover the inner surface of the ORC heat exchanger system. Electron-microscope exposures of *(b)* scale cross section morphology and *(c & d)* morphology and elemental analysis of the sulfide deposits and the barite matrix. Photos: 4a after Scheiber et al. (2014), 4c, b & d after Scheiber et al. (2012).

In the deep reservoir, the brine percolates the fractured granite which contains naturally a certain amount of radionuclides. These radionuclides are released in small concentrations to the circulating brine by rock-fluid interaction, Degering and Köhler (2009), Degering and Köhler (2011), Eggeling (2010) and Eggeling et al. (2013). Hereby, the activity of Ra-226 in the Soultz geothermal brine is about 30 Bq/kg, Eggeling et al. (2013). Scale related radionuclide uptake and accumulation is a result of chemical substitution of Ra-226 against Ba and Sr in the crystal lattice of strontium rich barite ($Ba_{0.6}Sr_{0.4}SO_4$) and of Pb-210 in the crystal lattice of galena (PbS)., e.g. Doerner and Hoskins (1925), Ceccarello et al. (2004), Curti et al. (2010), Kudryavskii and Rakhimova (2007) and Zielinski et al. (2001).The scales show only low specific activity, nevertheless they have to be classified as NORM (Naturally Occurring Radioactive Material) due to the presence of Ra-226 and Pb-210, Cuenot et al. (2013).

Four serious issues are connected with the precipitation of industrial scales, classified as NORM, in the surface installations of the Soultz power plant: Firstly, scales act as an insulation material in the tube heat exchanger which leads to a significant efficiency decrease in the heat transfer. In consequence, extensive time and cost consuming cleaning procedures had to be applied. Secondly, specific protection regulation for workers and for scale disposal needed to be followed due to the presence of radionuclides in the scales. Those scales are considered as radioactive waste deposits and had to be evacuated by ANDRA (French National Agency for Radioactive Waste Management). Thirdly, the inner diameter of the injection wells decrease slowly but continuously due to deposition of scales. Recently, well loggings proofed the existence of a progressing precipitation front inside of the injection wells versus depth which can possibly reach the open-hole section as a function of injected brine volume and brine temperature. Fourthly, dismantling and disposal of the surface installations rose to a cost and time intensive issue which was not considered at the first place.

To avoid scale formation and thereby radioactive contamination of deposits, several measures were developed in the past in the hydrocarbon producing industry. Most common method is the addition of scale inhibitors based on phosphonates, polyphosphates and polycarboxylates (He et al., 1994).

3. SCALE INHIBITOR SELECTION: LABORATORY TESTS

Strontium rich barite dominates the scales at the geothermal power plant of Soultz-sous-Forêts. For inhibition of this type of sulfate mineral, 4 chemical products based on different types of phosphonic acid were chosen to be tested for their effectiveness of scale mitigation at the Soultz geothermal site. Some parts of this study were also presented in Scheiber et al. (2013) and Scheiber et al. (2014).

3.1 Efficiency of phosphonate based Inhibitors

Phosphonates are well known scale inhibitors which are widely used in oilfield applications (Black et al., 1991 and He et al., 1994). They act in two different ways: On one hand they form water soluble complexes with specific metal ions. On the other hand, they inhibit crystal growth by adsorption on growth-active surfaces which leads thereby to retardation or blocking of the growth rate.

The degree of inhibitor efficiency relies on several physical-chemical parameters: pH, coordination number of the complex, thermal stability, adsorption affinity and the presence and concentration of co-ions like Ca^{2+}, Mg^{2+}, Sr^{2+} or Pb^{2+} in solution, the degree of oversaturation of barite as well as of the degree of oversaturation of the inhibitor.

With decreasing pH, the inhibiting efficiency of phosphonate on sulfate mineral growth, like barite or gypsum, also decreases (Van Rosmalen et al., 1980, He et al., 1994 and Rosenberg et al., 2012). Phosphonate in general can be very effective at very low concentrations. This type of threshold inhibition is related to phosphonate adsorption or adsorption of their dissociated compounds on growth-active surfaces (Weijnen and Van Rosmalen, 1986, He et al., 1996 and Pina et al., 2004). As a consequence of this processes, the crystal morphology changes from typically idiomorphic crystals to smoothed and rounded surfaces (Black et al., 1991 and Pina et al., 2004). A high concentration of co-ions can trigger the precipitation of metal-phosphonate (Nowak, 2003) and therefore inhibitor/brine compatibility tests are required before on-site application. With increasing temperature a higher amount of inhibitor is needed (He et al., 1994) and also thermal induced decomposition of the phosphonate needs to be considered. Thermal stability depends on the specific properties of the selected product.

Figure 5 shows the morphology of barite crystals which were formed by mixing NaCl, $NaSO_4$ and $BaCl_2$ to an artificial brine based on the TDS of the Soultz brine (Figure 5 left), see chapter 3.3. After adsorption of the scale inhibitor on growth-active barite surfaces (Figure 5 middle) the number and size of barite crystals decreased significantly (Figure 5 right).

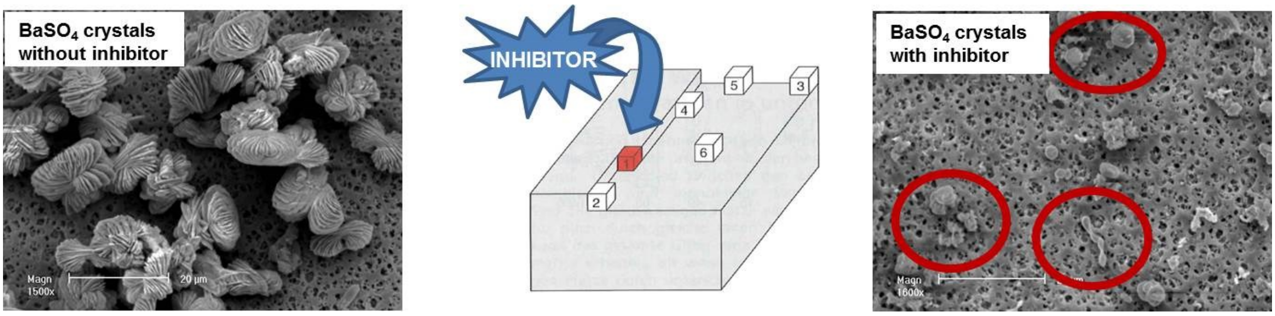

Figure 5: Mitigation of scale formation by adsorption of inhibitor molecules on growth active barite surfaces. *Left:* Morphology of barite crystals without inhibitor addition. *Middle:* Type of reaction for retardation or blocking of crystal growth by phosphonic acid, after Kleber (1990). *Right:* Morphology of barite crystals in the presence of a scale inhibitor.

3.2 Test of the Calciumtolerance

The Soultz brine contains 6.5 mg/l Ca in Na-Cl based brine with TDS close to 100 g/l. All 4 inhibitor products were tested for their ability to avoid coprecipitation of Ca-phosphates. Therefore, the products were added at 3 different concentrations, 0.5, 3 and 5% active concentration, to a Ba^{2+} and Sr^{2+} free *artificial brine (#1)*. Composition of artificial brine (#1), inhibitor concentration and results are listed in Table 2. Brine was produced in the same way as described for brine (#2). All brine/inhibitor mixtures kept a transparent state and therefore all products showed a good calcium tolerance.

Table 2: Composition of artificial brine (#1) and results of the calcium tolerance test with various inhibitor concentrations.

Artificial Brine (#1)		
Na in mg/l	Cl in mg/l	Ca in mg/l
25900	51520	6530
Results		
Product	*Concentration*	*Ca-Tolerance*
Inhibitor Green	0.5, 3 and 5%	good
Inhibitor Orange	0.5, 3 and 5%	good
Inhibitor Blue	0.5, 3 and 5%	good
Inhibitor Red	0.5, 3 and 5%	good

3.3 Efficiency Tests with Artificial Brine

For efficiency tests, the four products were mixed with *artificial brine (#2)*, Table 3. The brine was created by adjusting a Na-Ca-Sr-Cl stock solution which was mixed with Na_2SO_4 and $BaCl_2$ solution. The Ba^{2+} concentration was adjusted 2.3 times higher and the SO_4^{2-} concentration was adjusted 4 times higher than in the original Soultz brine to speed up barite formation by increasing the level of oversaturation.

Table 3: Composition of artificial brine (#2), used for inhibitor efficiency tests.

Artificial Brine (#2)					
Na (mg/l)	Ca (mg/l)	Ba (mg/l)	Sr (mg/l)	Cl (mg/l)	SO_4 (mg/l)
25430	6340	60 (overdose)	400	50770	1010 (overdose)

Active content of 5 and 15 mg/l respectively of Inhibitor Green, Red, Blue and Orange were tested for barite mitigation. Inhibitor products were added directly to the Na-Ca-Sr-Cl stock solution which was mixed with solutions of Na_2SO_4 and $BaCl_2$. The samples were mixed continuously at 125 rpm (revolutions per minuets) for 48 h at 60°C. Barite formation was detected using turbidity measurements. To confirm these results, additional measurements with ICP-MS (DIN 38406 E29) were performed for Ba, Ca, Sr detection for brine samples which were taken after 6 and 48 h as well as IC measurements (DIN EN ISO 1034-2) for SO_4 detection.

The effectiveness of Inhibitor Green, Inhibitor Red, Inhibitor Blue and Inhibitor Orange are compared to barite formation in inhibitor-free brine, Figure 6. Barite formation in inhibitor-free brine started immediately after mixing (black solid line) and Ba^{2+} concentration decreased from 60 to 20 mg/l within the first 48 h. Independent of inhibitor active concentration of Inhibitor Green (grey dashed line), the Ba^{2+} concentration dropped even faster than in inhibitor-free brine. It is not clear why this product triggered the barite formation but it was withdrawn immediately from the laboratory study. Inhibitor Red and Blue (light grey solid line and grey solid line) showed a slightly better performance at an active concentration of 15 mg/l but at both concentrations the Ba^{2+} concentration did not drop below 50 mg/l within 48 h. Inhibitor Orange (dark grey solid line) mitigate barite formation at best at 15 mg/l active concentration, no barite was formed during the first 24 h. Afterwards, Ba^{2+} concentration decreased quite fast. At 5 mg/l active concentration, barite formation was nearly mitigated during the first 6 h and afterwards Ba^{2+} concentration decreased to 36 mg/l. Based on this experiment, Inhibitor Blue showed the best performance.

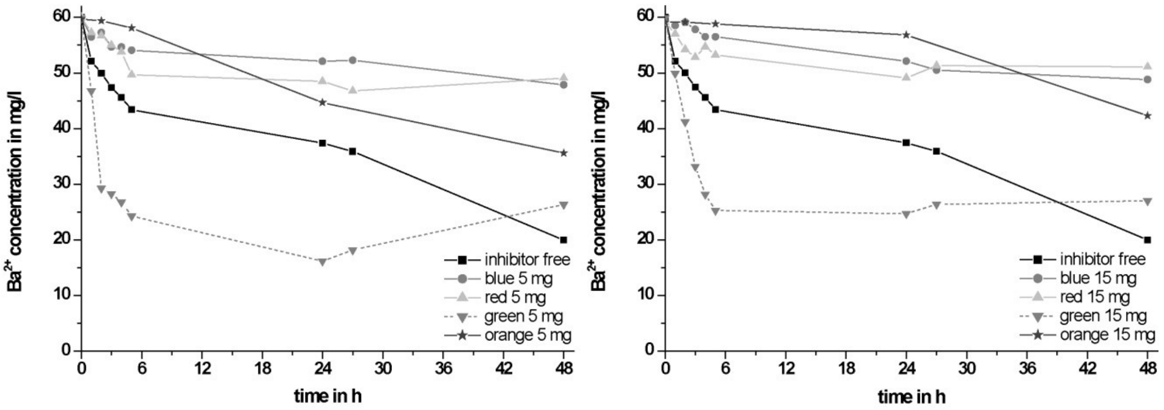

Figure 6: Ba^{2+} concentration as a function of time after addition of Inhibitor Green (grey dashed line), Inhibitor Red (light grey solid line), Inhibitor Blue (grey solid line) and Inhibitor Orange (dark grey solid line). The black solid line represents barite formation in Inhibitor-Free brine. *Left:* Inhibitor active concentration of 5 mg/l, extended after Scheiber at al. (2013) and Scheiber et al. (2014). *Right:* Inhibitor active concentration of 15 mg/l.

After 48 h the efficiency tests ended and brine/inhibitor mixtures were filtered through 0.45 µm cellulose acetate filters, washed with demineralized water and dried at room temperature. Morphology of filter remains was investigated by electron microscopy after gold sputtering using a Phillips XL 20 device.

Filter remains of the inhibitor-free brine covered more than 50% of the filter surface and a lot of barite crystals, twinned and radiating rose-like aggregates of up to 20 µm sizes, were distributed homogenously, Figure 7. All inhibitors retarded but did not block barite formation. Filter remains of Inhibitor Red and Blue covered less than 10% of the filter surface whereas more barite crystals were formed in the presence of Inhibitor Orange which is in good accordance with Ba^{2+} analysis after 48 h. All crystals formed were significantly smaller than in the absence of a scale inhibitor but the impact of morphology differ strongly. Inhibitor Red retards partially crystal growth but still small scale rose-like aggregates were formed. In case of Inhibitor Blue, tiny and twinned barite crystals with plate like morphology are present. Inhibitor Orange had the strongest impact on crystal morphology only small scale barite particles with size of maximum 5 µm were formed showing sphere like or dumbbell shaped surfaces.

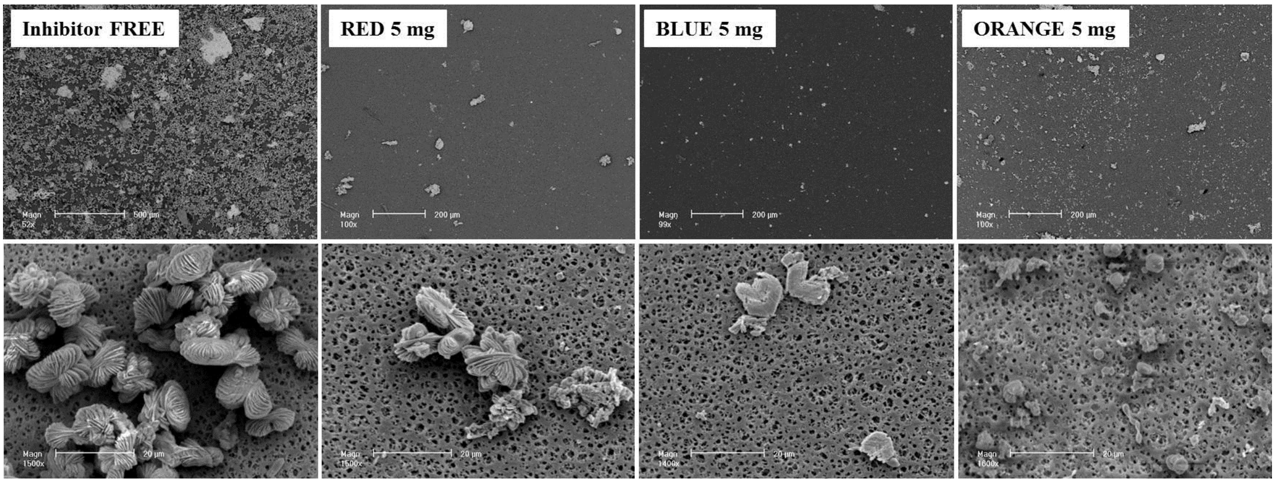

Figure 7: Electron microscope exposures of filter remains of the laboratory efficiency experiments: Filter surface coverage and morphology of barite crystals of Inhibitor-free brine *(left)*, Inhibitor Red *(middle, left)*, Inhibitor Blue *(middle right)* and Inhibitor Orange *(right)* after 48 h experiment duration.

3.4 Efficiency Tests with Original Soultz Brine

After determination of calcium tolerance and inhibitor efficiency in artificial brines, the remaining three products, Inhibitor Red, Blue and Orange, were tested for their barite inhibition effectiveness in the Soultz brine. Therefore, closed bottle tests were performed. This experiment was already described in detail in Scheiber et al. (2013) and Scheiber et al. (2014). Here, the morphology study is added to emphasize the impact of inhibitor products on crystal shape.

Original Soultz brine was sampled at the 6th April 2011 at the production well GPK-2 by cooling the brine from160˚C to70˚C in a small scale tap-water cooled device. Chemical composition of the brine is presented in Table 1. Inhibitor products were added immediately after sampling with an active concentration of 5 mg/l. Bottles were stored at room temperature for 8 days. Afterwards, the inhibitor/brine samples were filtrated and the filtrate was analyzed for Ba, Sr, Ca concentration by ICP-MS (DIN 38406 E29) and SO_4 (DIN EN ISO 1034-2). Filter residues were investigated visually and by electron microscopy after gold sputtering, using a Phillips XL 20 device equipped with a JEOL JXA-840 A, an EDX application for determination of the elemental composition.

The Ba^{2+} concentration decreased from 26 to 16 mg/l within the Inhibitor-Free brine during 8 days. Nearly no decrease was observed for Inhibitor treated brine samples. Chemical composition and morphology of the filter residues of the inhibitor treated brine and non-treated brine differed strongly. In the Inhibitor-Free brine, a lot of plate-like idiomorphic barite crystals were formed up to several 10th µm sizes. Additionally, some co-precipitates of iron oxides/hydroxides are present due to the oxygen uptake during on-site sampling, Figure 8 left. Inhibitor Red suppressed co-precipitation and only some tiny barite crystals were formed. These crystals reached a maximum size of 5-10 µm in diameter and showed no idiomorphic plate-like shape, Figure 8 middle-left. Inhibitor Blue also mitigated barite precipitation successfully but allowed formation of some more barite crystals to be formed in comparison to Inhibitor Red, co-precipitation was blocked completely, Figure 8 middle-right. Inhibitor Orange did not suppress co-precipitation at all but contrary to the efficiency tests with artificial brine it mitigated barite formation in the Soultz brine for 8 day with the best efficiency of all inhibitors. Only very few barite crystals with sizes <5µm were formed, Figure 8 right.

A few remarks should be added concerning development of significant differences of crystal morphology in artificial brine and original Soultz brine. Twinned and radiating rose-like barite crystals with sizes of up to 20 µm were formed in artificial brine at 60°C during 2 d whereas plate-like crystals originated in Soultz brine at 60°C during 8 d, forming solid solutions of strontium rich barite. Two different parameters could be responsible for this. First, the oversaturation state of the artificial brine was 2.3 times higher than the one of original Soultz brine. This affects directly crystallization kinetics and speeds up crystal growth of barite surfaces with high natural growth rates. In consequence, the slow growing surfaces dominate morphology. Second, in solid solutions of barite-celestine mixed crystals, the ratio of the end members can affect morphology significantly. Due to the oversaturation of barium in the artificial solutions, a lot of crystals, formed from artificial brine, showed a higher ratio of barium against strontium than in crystals which were formed from originally Soultz brine. Other parameters also may influence crystal shape like the presence of co-ions.

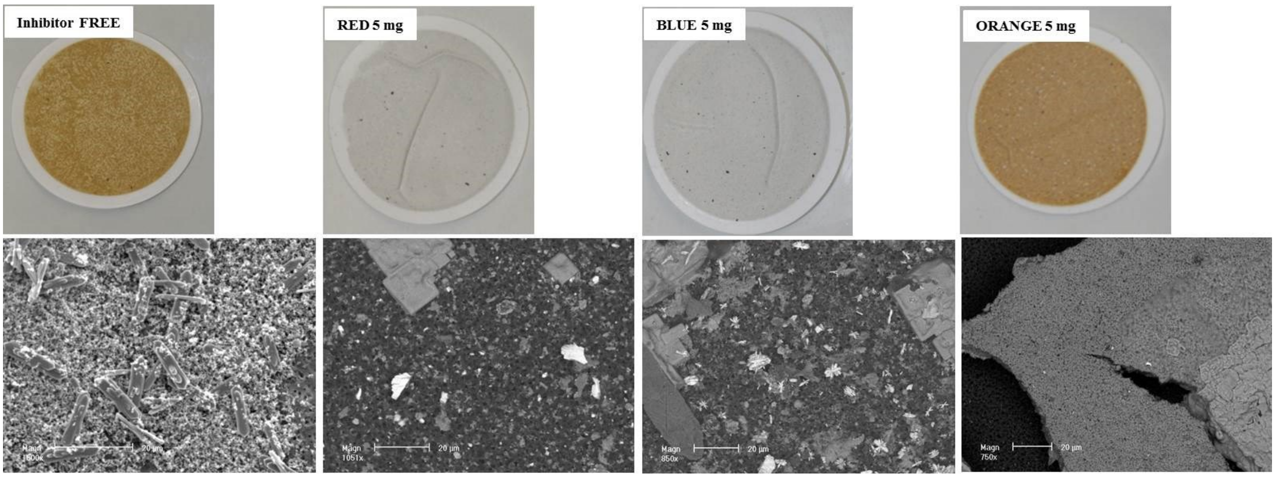

Figure 8: Filter residues of inhibitor efficiency tests, involving original Soultz brine, are compared with electron microscope exposures of these filter residues. Inhibitor-free brine: Barite crystals are embedded in a fine grained iron oxide/hydroxide matrix *(left)*. Inhibitor Red and Blue: Single barite crystals are visible *(middle-left & middle-right)*. Inhibitor Orange: Very few, tiny barite crystals are embedded in a fine grained iron oxide/hydroxide matrix *(right)* after 8 d experiment duration. Photos of the entire filters after Scheiber at al. (2013) and Scheiber et al. (2014).

3.5 Inhibitor selection

Inhibitor Green, Red, Blue and Orange showed a very different performance during the laboratory test. Inhibitor Green even triggered barite formation and was therefore removed from the study. Inhibitor Orange showed the strongest impact on barite morphology, indicating thereby a very high affinity for adsorption on crystal surfaces and blocking of crystal growth. Unfortunately the long-term performance of this inhibitor is not as strong as for Inhibitor Red and Blue in test involving artificial brine. Even with the higher dose rate of 15 mg/l active concentration the total scale mitigation was worse than for Inhibitor Red and Blue at 5 mg/l after 48 h. Moreover, Inhibitor Orange showed no tendency to mitigate co-precipitation during the efficiency tests with original Soultz brine. Contrary, both Inhibitors, Red and Blue, managed to suppress co-precipitation. Concerning barite mitigation in original Soultz brine Inhibitor Red showed a slightly better performance than Inhibitor blue, fewer crystals were formed in presence of Inhibitor Red.

Inhibitor Red was selected for on-site tests. This product is based on DTPMP (Diethylenetriaminepentakis (methylene-phosphonic acid)). Before on-site application, dose rate adjustment was conducted by tube blocking tests and laboratory studies concerning rock/inhibitor interaction were continued.

3.5 Dose Rate Adjustment

For dose rate adjustment, dynamic tube blocking test were performed in order to determine the required dose rate for the Soultz brine. For this type of test, brine/inhibitor mixtures flow continuously through capillary tubes of small diameters. If scales are formed at tube surface, the inner diameter decreases and the pressure rise. The differential pressure is monitored by measuring the pressure before entering and after leaving the capillary tube. Every experiment starts with a pre-scale test. Inhibitor-free brine flows through the capillary tube and the blocking time is detected. This is the minimal blocking time which should be elongated significantly by adding different concentration of inhibitor.

All experiments were conducted at 60˚C which is the minimal injection temperature of the Soultz injection wells. The barite solubility decreases with decreasing temperature, Blount (1977), which means that for the Soultz injection conditions the lowest solubility will be reached at 60°C temperature and the inhibitor has to operate at its maximum efficiency. Artificial brine was used for the tube blocking tests and barium, strontium and sulfate concentration were adjusted to an oversaturated state of strontium-rich barite to decrease nucleation time. Composition of artificial brine (#3) is listed in Table 4. The artificial brine was produced in the same way as described for brine (#2). Inhibitor Red only was tested with tube blocking tests.

Table 4: Composition of the artificial brine (#3) for dynamic tube blocking tests

Artificial Brine (#3)					
Na (mg/l)	Ca (mg/l)	Ba (mg/l)	Sr (mg/l)	Cl (mg/l)	SO_4 (mg/l)
28380	7800	300 (overdose)	2050 (overdose)	58090	1860 (overdose)

With increasing inhibitor concentration, blocking time of the capillary tube increased, Figure 9. At low inhibitor concentration of 5 and 25 ppm/l, barite scale was formed immediately and tubes got blocked within 25 min. With increasing inhibitor concentration, the dynamic operation time increased significantly. The best performance was observed for an inhibitor concentration of 45 ppm. Here, scaling was mitigated successfully for 2 h. Based on the degree of barite oversaturation in artificial brine (#3), the optimal dosage for the Soultz conditions was calculated to be 4 mg/l active content of Inhibitor Red per liter of geothermal brine.

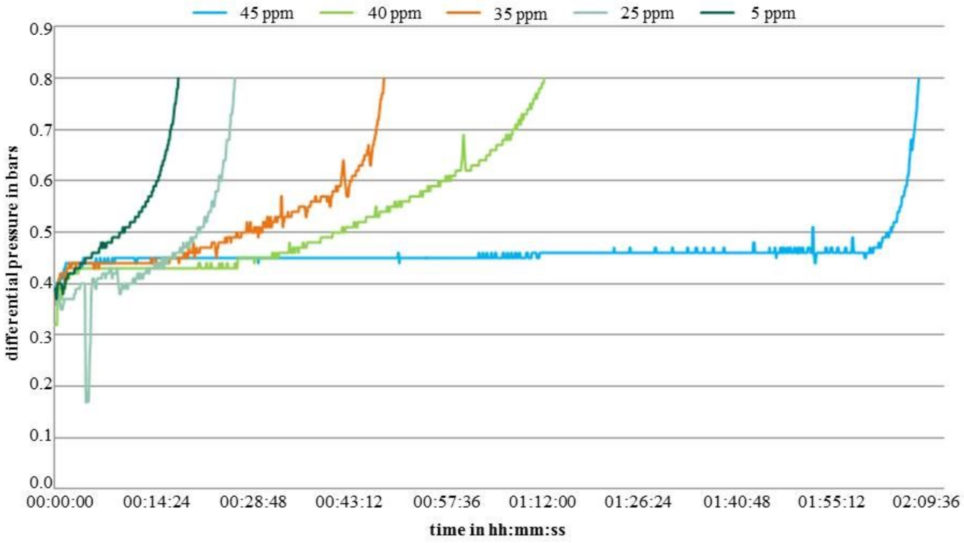

Figure 9: Dynamic tube blocking tests with DTPMP based inhibitor: active content of 5 ppm (dark blue curve), 25 ppm (light blue curve), 35 ppm (orange curve), 40 ppm (green curve) and 45 ppm (blue curve) of Inhibitor Red are displayed as a function of the differential pressure (y-axis) versus time (x-axis), after Scheiber at al. (2013) and Scheiber et al. (2014).

3.5 Host Rock/Inhibitor Interaction

Investigations of the inhibitor performance at surface installations conditions are important for best effectiveness adjustment of scale mitigation in the heat exchanger system. However, inhibitor performance in the subsurface installations, injection wells, open-hole section and near-wellbore region also needs to be considered. During long-term circulation, cold brine is injected for several month or years into the injection wells. Thereby, a cooling front in the well and around the open-hole section will spread out as a function of injected brine volume and brine temperature.

At Soultz, the reservoir permeability is related to fractures with thicknesses of µm to cm in the deep reservoir. After passing the heat exchanger unit, the inhibitor has to keep up its good performance in the injection wells and in the cooling region around the wellbore until injected brine is heated up to a level were rock-fluid equilibrium is reached. Moreover, secondary mineral formation by inhibitor/host rock (granitic) interactions or inhibitor/fracture fillings interactions have to be avoided.

Parameters, long-term efficiency and secondary mineral precipitation by inhibitor/host rock interactions were investigated in laboratory experiments.

3.5.1 Material selection of the granitic host rock

Two different host rocks of the Soultz granitic reservoir were selected: one piece from a shallow and hydrothermal altered part of the reservoir (depth: 1674 m, core of the exploration well EPS-1) and cuttings from the open-hole section of GPK-2 which is dominated by a fractured two mica granite (several samples between 4767 and 4780 m depth), Figure 10. The cutting samples were selected based on the presence of fracture zones. Host rock and fracture fillings can show a very different mineralogy, therefore, the interaction of the inhibitor with both, host rock and fracture fillings needs to be considered.

Figure 10: Host rock material of the Soultz granitic reservoir: Cuttings from GPK-2 (appr. 4775 m depth) and a piece of core from EPS-1 (1674 m depth), after Scheiber at al. (2013) and Scheiber et al. (2014).

3.5.2 Batch experiment setup and results

For batch experiments, artificial brine (#4) was mixed with grinded powder of reservoir rocks. The composition of this brine is listed in Table 5. Brine was produced in the same way as described for brine (#2).

Table 5: Composition of artificial brine (#4) for host rock–inhibitor interaction experiments.

Artificial Brine (#4)					
Na (mg/l)	Ca (mg/l)	Ba (mg/l)	Sr (mg/l)	Cl (mg/l)	SO_4 (mg/l)
2839	7800	60 (overdose)	400	57930	370 (overdose)

The barite formation and reservoir rock mineralogy was investigated in the presence of Inhibitor Red as well as in the absence of the inhibitor. Therefore, host rock material from two different Soultz reservoir depths was grinded to powder. Respectively 10 g of powder was mixed with 150 ml artificial brine (#4) at 60°C in tinplate capsules (5 per experiment) which were sealed and immediately heated up to 90°C. The samples were regularly mixed by shaking. As a function of time, respectively 2, 6, 24, 72, 168 h, tinplate capsules were removed from the experiment, unsealed and filtrated. Filter residues were dried and investigated by X-ray diffraction (XRD) and Scanning Electron Microscopy (SEM). Ba^{2+}, Sr^{2+}, SiO_2, SO_4^{2-} and PO_4^{3-}concentrations were determined in the filtrate.

In the absence of Inhibitor Red, the Ba^{2+} concentration started to decrease immediately after start of the experiment and reached a constant level of 6 mg/l after 3 days, Figure 11 dashed lines. In the presence of Inhibitor Red, the Ba^{2+} concentration was constant during the first 24 h and decreased continuously but slowly during the experiment, Figure 11 solid lines. The two reservoir rocks showed the same behavior with or without inhibitor, their presence had no direct impact on the Ba^{2+} concentration. Mineralogical composition did not change with time in the presence of the inhibitor. Secondary mineral formation by inhibitor-reservoir rock interaction experiments was only observed for barite but not for phosphate minerals, nor by XRD neither by SEM analysis.

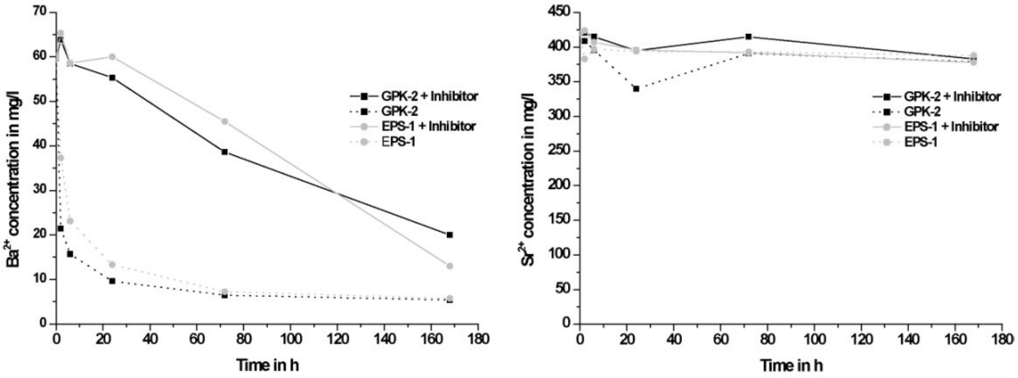

Figure 11: Batch experiments for reservoir rock- inhibitor interaction with artificial brine (#4). Ba^{2+} concentration as a function of time in the presence of Inhibitor Red (solid lines) and in the absence of the inhibitor (dashed lines). After Scheiber at al. (2013) and Scheiber et al. (2014).

PO_4^{3-} concentration in the filtrate was analyzed as a function of time. By thermal decomposition of the phosphonic-acid, PO_4^{3-} is formed and can be used as an indicator for decomposition processes. No significant increase of the ortho-phosphate concentration was observed during the batch experiment. Nevertheless, the decrease of the Ba^{2+} concentration and precipitation of barite starts after 24 h, Figure 11 solid lines. Two theories could explain this effect. First, the growth of barite crystals takes place at surfaces with non-preferred adsorption sides for the phosphonic-acid but growth rate is very low. Second, a fraction of the phosphonic-acid adsorbed on minerals surfaces of the reservoir minerals and was not available for barite mitigation which allowed growth-active barite surfaces to growth. Further investigations are required to clarify this point.

4. ON-SITE TEST OF THE SCALE INHIBITOR

After successful selection of the inhibitor in laboratory experiments, the product was tested on-site at in-situ conditions for its efficiency of scale avoidance at the 6th February 2013. Parts of this study was also presented in Scheiber et al. (2013) and Scheiber et al. (2014).

4.1 Design and Installation of the Inhibitor Injection System

An injection of the inhibitor at the production side at approximately 160°C is necessary to guarantee appropriate mixing with the geothermal fluid before entering the heat exchanger units. Therefore, the inhibitor is injected at the hot side of the production side approximately 8 m downstream of the production well and 20 m before entering the heat exchangers. The selected product for scale inhibition, Inhibitor Red, has a boiling point of 110°C. The addition of the inhibitor at the production side risks decomposition of a fraction of the injected inhibitor. Nevertheless, a complete mixing of the inhibitor with the brine before entering the heat exchanger (before nucleation of barite seeds) is required to guarantee best results.

A flange-mounted pipe is connected to the main production pipe. Within this flange, hastelloy coiled tubing is installed and its tip is placed in the center of the production pipe. Here the inhibitor is added drop-wise to the geothermal fluid at 20 bars and 155°C.

4.2 On-site efficiency test of the inhibitor injection

The inhibitor was added continuously to the production stream of the geothermal brine. The optimum dosage for the Soultz conditions was determined by dynamic tube blocking tests to be 4 mg/l active content at 60°C. However, the dose-rate of the inhibitor was adjusted to an active content of 7.6 mg/l to compensate partly decomposition of the inhibitor due to its boiling point, which is below production temperature.

The operation conditions of the Soultz geothermal power plant at the time of inhibitor injection were 155°C/21 bars at a flow rate of 15.3 l/s at the production side and 70°C/18 bars with a flow rate of 15 l/s at the injection side. The power plant was still in the restart phase after a maintenance period, therefore, temperature and flow rate of the production stream were not at their maximum and a certain amount of suspended solids were present in the productions stream.

During inhibitor injection, the Ba^{2+} concentration kept a constant level of 26 mg/l from production to re-injection. Chemical composition of the brine is listed in Table 1. Sr^{2+} and SO_4^{2-} concentration decreased slightly which can also be related to the analysis error of the applied methods. Pb^{2+} concentration increases from 0.07 mg/l at the production side to 0.1 mg/l at the re-injection side. It is possible that due to the slight overdose of the inhibitor, pre-existing scaling of Galena (PbS), which is attached to pipe surfaces, was partly dissolved. This finding has to be re-produced to confirm this theory. A slight decrease of the pH from 4.88 to 4.82 can be related to the injection of phosphonic-acid which has a pH < 2 at its concentrated state. The Eh value increased from 5 to 117 mV (SHE) which can be caused by electrochemical processes.

Immediately after fluid sampling, a filter station was connected to the sampling station and in-situ filtration at 4- 6 bar was applied. Brownish and very fine grained particles covered the full filter surfaces after filtration of 1 liter brine, Figure 12. Filters and filter residues were washed with demineralized water and dried at room temperature for analysis by Scanning Electron Microscopy (SEM).

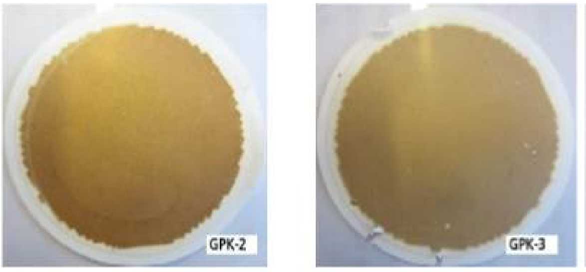

Figure12: Filter residues after on-site filtration at the production well GPK-2 and the injection well GPK-3 during inhibitor injection, after Scheiber at al. (2013) and Scheiber et al. (2014).

Scanning Electron Microscopy (SEM) (Philips XL 20) equipped with an EDX system (Hitachi S-520) for elemental analysis was applied in order to detect newly formed barite precipitates if present. Semi-quantitative elemental analysis was conducted at filter sections of 1100 x 880 µm, Table 6.

Table 6: Comparison of the elemental composition of filter residues of production and injection side after in-situ filtration.

Filter residues production side GPK-2	Filter residues injection side GPK-3
oxides/sulfides of Cu (38%) Pb (25%), As (17%), Sb (11%), Fe (9%)	*oxides/sulfides of* Cu (53%) Fe (11%), As (13%), Ba (13%)

The comparison of elemental analysis showed that at production side the oxide/sulfide matrix is dominated by Cu, Pb, As and Sb whereas the filter residues at the injection side are dominated by Cu, Fe, As and Ba. Based on the oxygen to sulfur ratio, the matrix is dominated by oxides and contains a minor amount of sulfides. Either the oxide/sulfide particles are produced from the well and transported as suspended matter through the surface installations of the power plant or the particles precipitated during filtration in case of oxygen pollution during sampling. Very interestingly is the high amount of Cu inside of both filter residues and the low Pb concentration at the injection side. A precipitation of Cu-oxide/sulfide during filtration is not very likely due to the low amount of dissolved Cu in the production brine, Table 1. It is possible that some subsurface equipment released Cu particles by abrasion and/or corrosion processes and it is possible that those particles got trapped during filtration. Further investigations are required for this topic.Low concentrations of Pb-rich particles at the injection brine can be explained either by dissolution processes of suspended particles, as already discussed, or by settling of suspended fines at locations of reduced flow.

Very few particles of barite were found in filter residues of the injection side. In the beginning it was not clear if particles were formed during current circulation or if their appearance is related to former production periods where no inhibitor was injected. Based on the fluid analysis, Table 1, no decrease of the Ba^{2+} concentration was monitored and barite crystals show idiomorphic morphology. Adsorption of phosphonic-acid on growth active surfaces changes particle size and to some extend also barite morphology but these types of changes were not observed. In correlation with the findings of the fluid chemistry it is concluded that the particles were formed during earlier production periods. Based on these results no precipitation of strontium rich barite takes place by cooling of geothermal fluid in the heat exchanger units. Inhibitor Red successfully blocked the growth of barite crystals.

5. CONCLUSIONS

Scales are formed in surface installations of the geothermal power plant in Soultz-sous-Forêts due to the temperature decrease at the heat exchanger system. Strontium rich barite ($Ba_{0.6}Sr_{0.4}SO_4$) dominates the deposits but also a minor fraction of galena (PbS) and some traces of As, Sb, Fe-mixed sulfides are formed. Scales have to be classified as NORM due to the incorporation of radionuclides, Ra-226 into barite and Pb-210 into galena. A scaling inhibitor was selected in laboratory experiments out of various products and was successfully tested for its efficiency at the power plant after installation of the injection system. Barite precipitation was successfully suppresses during a short-term test.

Small-scale laboratory experiments were found to be simple but powerful tools for successful selection of scale inhibitors for geothermal power plants. Based on the respective brine composition, the optimum product can be selected and dose rate can be adjusted. The methods of the laboratory study involved pre-tests with several artificial brines. Parameters like calcium tolerance, effectiveness, dose rate adjustment, thermal stability and rock/brine/inhibitor interaction have been successfully investigated with artificial brines. Those brines were mixed based on the main components and on Total Dissolved Solids (TDS) of original Soultz brine. Different degrees for barite oversaturation were adjusted. It turned out that one of the inhibitor even triggered barite formation and was therefore removed from the study. For the final product selection, original brine was used. Here, the real effectiveness and the capability to avoid co-precipitation were successfully investigated. It was found that the inhibitor which changes morphology most can be considered as very reactive and possessing a strong affinity for adsorption on barite surfaces. Interestingly, this does not necessarily imply that this one is also the most efficient one for long-term barite scale inhibition. Efficiency tests in artificial brine showed that this type of inhibitor is most efficient during the first few hours and efficiency can be elongated by dose rate increase. The issue of long-term efficiency becomes important by considering that not only the surface installations needs to be protected from scale formation and deposition at the Soultz site but also the injection wells, the open-hole sections and the near wellbore region of the fractured reservoir needs also to be protected due to the progressing precipitation front. Therefore, the selected barite scale inhibitor needs to perform well for at least 24 h in order to allow the brine to heat up. The most reactive inhibitor product, Inhibitor Orange, did perform best during the first few hours but after 6 h, efficiency decreased very fast. The remaining Inhibitors Red and Blue showed a slightly lower performance in the first few hours but were able to mitigate barite scale formation efficiently during the first 24 h.

All in all, four different inhibitor products were tested. All products showed a very high calcium tolerance but different performances for barite scale inhibition and inhibition of co-precipitates in artificial and original Soultz brine. The most successful inhibitor product for the Soultz location is based on DTPMP (Diethylenetriaminepentakis (methylene-phosphonic acid)). The on-site injection test at the power plant worked out very well. Barite formation can be significantly retarded in the future and time periods between cleaning operations of the heat exchanger units are expected to increase. Moreover, tests of long-term efficiency at injection conditions and thermal stability showed very promising results for successful protection of injection wells, open-hole section and near-wellbore region by inhibitor injection at the surface installations.

ACKNOWLEDGEMENTS

This work was supported by BGR, BMU and Forschungszentrum Jülich (Germany), ADEME (France) and by a consortium of French and German industrial members (EDF, EnBW, ES, Pfalzwerke, Steag). The technical team of the GEIE is also greatly acknowledged for their support during installation of the inhibitor system and during on-site tests. We like to thank the company Zschimmer & Schwarz for conducting the tube blocking tests.

REFERENCES

Aquilina, L., Pauwels, H., Genter, A. and Fouillac, C.: Water-rock interaction processes in the Triassic sandstone and the granitic basement of the Rhine Graben: Geochemical investigation of a geothermal reservoir, *Geochimica et Cosmochimica Acta*, **61**, (1997), 4281-4295.

Black, S., Bromley, L., Cottier, D., Davey, R., Dobbs, B. and Rout, J.: Interactions at the Organic/Inorganic Interface: Binding Motifs for Phosphonates at the Surface of Barite Crystals, *Journal of the Chemical Society, Faraday Transactions*, **87**, (1991), 3409-3414.

Blount, C.W.: Barite solubilities and thermodynamic quantities up to 300˚C and 1400 bars, *American Mineralogist*, **62**, (1977), 942-957.

Ceccarello, S., Black, S., Read, D. and Hodson, M.E.: Industrial radioactive barite scale: suppression of radium uptake by introduction of competing ions, *Minerals Engineering*, **17**, (2004), 323-330.

Curti, E., Fujiwara, K., Iijima, K., Tits, J., Cuesta, C., Kitamura, A., Glaus, M.A. and Müller, W.: Radium uptake during barite recrystallization at 23 ± 2˚C as a function of solution composition: An experimental ^{133}Ba and ^{226}Ra tracer study, *Geochimica et Cosmochimica Acta*, **74**, (2010), 3553-3570.

Cuenot, N., Scheiber, J., Moeckes, W., Guéry, B., Bruzac, S., Sontot, O., Meneust, P., Maquet, J., Orsat, J. and Vidal, J.: Evolution of natural radioactivity within the Soultz geothermal installation, *Proceedings*, European Geothermal Congress, Pisa, Italy, (2013).

Degering, D. and Köhler, M.: Natürliche Radionuklide in Anlagen der tiefen Geothermie, *Proceedings*, Geothermiekongress Bochum, Bochum, Germany, (2009).

Degering, D. and Köhler, M.: Gamma-spectrometric analysis of high salinity fluids – how to analyze radionuclides of the thorium decay chain far from radioactive equilibrium?, *Applied Radiation and Isotopes*, **69**, (2011), 1613-1617.

Doerner, H.A. and Hoskins, W.M.: Co-Precipitation of Radium and Barium Sulfates, *J. Am. Chem. Soc.*, **47**, (1925), 662-675.

Eggeling, L.: Auswirkungen der Nutzung salinarer Tiefenwässer auf den Betrieb der Geothermieanlage Bruchsal und Soultz-sous-Forêts unter besonderer Berücksichtigung natürlicher Radionuklide, *Bachelorarbeit*, KIT-AGW, September 2010, (2010), 52 pp.

Eggeling, L., Genter, A., Kölbel, T. and Münch. W.: Impact of natural radionuclides on geothermal exploitation in the Upper Rhine Graben, *Geothermics*, **47**, (2013), 80-88.

He, S., Oddo, J. and Tomson, M.: The inhibition of gypsum and barite nucleation in NaCl brines at temperatures from 25 to 90˚C, *Applied Geochemistry*, **9**, (1994), 561-567.

He, S., Kan, A. and Tomson, M.: Mathematical Inhibitor Model for Barium Sulfate Scale Control, *Langmuir*, **12**, (1996), 1901-1905.

Genter, A. and Traineau, H.: Hydrothermally altered and fractured granite as an HDR reservoir in the EPS-1 borehole, Alsace, France, *Proceedings,* 17th Workshop on Geothermal Reservoir Engineering, Stanford University, Stanford, CA, (1992).

Genter, A., Evans, K.F., Cuenot, N., Fritsch, D. and Sanjuan, B.: Contribution of the exploration of deep crystalline fractured reservoir of Soultz to the knowledge of Enhanced Geothermal Systems (EGS), *Geoscience*, **342**, (2010), 502-516.

Gérard, A. and Kappelmeyer, O.: The Soultz-sous-Forêts project: Proceedings of the first EEC/US workshop on geothermal Hot dry Rocks Technology, *Geothermics*, Special issue, (1987), 393-399.

Gérard, A., Genter, A., Kohl, T., Lutz, Ph., Rose, P. and Rummel, F.: The deep EGS (Enhanced Geothermal System) project at Soultz-sous-Forêts (Alsace, France), *Geothermics*, **35**, (2006), 473-483.

Kleber, W.: Einführung in die Kristallographie, 17th Edition, Berlin, (1990), pp. 416.

Kudryavskii, Yu.P. and Rakhimova, O.V.: "Coprecipitation of Radium with Barium Sulfate from Salt Solution", *Radiochemistry*, **49**, (2007), 541-544.

Nitschke, F.: Geochemische Charakterisierung des geothermalen Fluids und der damit verbundenen Scalings in der Geothermieanlage Soultz sous Forêts, *Masterthesis*, Institut für Mineralogie und Geochemie (IMG) at Karlsruher Institut of Technology (KIT), (2012), 126 pp.

Nowack, B.: Environmental chemistry of phosphonates, *Water Research*, **37**, (2003), 2533-2546.

Pauwels, H., Criaud, A., Vuataz, F-D., Brach, M. and Fouillac, C.: Uses of chemical tracers in HDR reservoir studies, examples of Soultz-sous-Forêts (Alsace, France), *Geotherm. Sci. Tech.*, **3**, (1991), 83-103.

Pauwels, H., Fouillac, C. and Fouillac, A-M.: Chemistry and isotopes of deep geothermal saline fluids in the Upper Rhine Graben: Origin of compounds and water-rock interactions, *Geochimica and Cosmochemica Acta*, **57**, (1993), 2737-2749.

Pina, C.M., Putnis, C.V., Becker, U., Biswas, S., Carrol, E.C., Bosbach, D. and Putnis, A.: An atomic force microscopy and molecular stimulations study of the inhibition of barite growth by phosphonates, *Surface Science*, **553**, (2004), 61-74.

Rosenberg, Y., Reznik, I., Zmora-Nahum, S. and Ganor, J.: The effect of pH on the formation of a gypsum scale in the presence of a phosphonate antiscalant, *Desalination*, **284**, (2012), 207-220.

Sanjuan, B., Millot, R., Dezayes, Ch. and Brach, M.: Main characteristics of the deep geothermal brine (5 km) at Soultz-sous-Forêts (France) determined using geochemical and tracer test data, *C. R. Geoscience*, **342**, (2010), 546-559.

Sanjuan, B., Brach, M., Béchu, E., Touzelet, S., Crouzet, C. and Jean-Prost, V.: Soultz EGS plant exploitation – Phase III: Scientific program about on-site operations of eochemical monitoring and tracing (2010-2013), *First yearly progress report BRGM/RP-59902-FR*, (2011), 92 pp.

Scheiber, J., Nitschke, F., Seibt, A. and Genter, A.: Geochemical and Mineralogical Monitoring of the Geothermal Power Plant in Soultz sous Forêts, (France), *Proceedings*, 37rd Workshop on Geothermal Reservoir Engineering, Stanford University, Stanford, California, USA, (2012).

Scheiber, J., Seibt, A., Birner, J., Genter, A. and Moeckes, W.: Application of a Scaling Inhibitor System at the Geothermal Power Plant in Soultz-sous-Forêts: Laboratory and On-Site Studies, *Proceedings*, European Geothermal Congress, Pisa, Italy, (2013).

Scheiber, J., Seibt, A., Birner, J., Cuenot, N., Genter, A. and Moeckes, W.: Barite Scale Control at the Soultz-sous-Forêts EGS site, *Proceedings*, 38rd Workshop on Geothermal Reservoir Engineering, Stanford University, Stanford, California, USA,, (2014).

Van Rosmalen, G., Van der Leeden, M. and Gouman, J.: The Influence of Inhibitors on the Growth of Barium Sulfate Crystals in Suspension: Scale Prevention (II), *Kristall und Technik*, **15**, (1980), 1269-1277.

Weijnen, M. and Van Rosmalen, G.: Adsorption of Phosphonates on Gypsum Crystalls, *Journal of Crystal Growth*, **79**, (1986), 157-168.

Zielinski, R.A., Otton, J.K. and Budahn, J.R.: Use of radium isotopes to determine the age and origin of radioactive barite at oil-field production sites, *Environmental Pollution*, **113**, (2001), 299-309.